Plant, Cell & Environment

Plant, Cell and Environment (2014) **37**, 2679–2690 doi: 10.1111/pce.12408

Original Article

Coordination between water transport capacity, biomass growth, metabolic scaling and species stature in co-occurring shrub and tree species

Duncan D. Smith & John S. Sperry

Department of Biology, University of Utah, Salt Lake City, UT 84112, USA

ABSTRACT

The significance of xylem function and metabolic scaling theory begins from the idea that water transport is strongly coupled to growth rate. At the same time, coordination of water transport and growth seemingly should differ between plant functional types. We evaluated the relationships between water transport, growth and species stature in six species of co-occurring trees and shrubs. Within species, a strong proportionality between plant hydraulic conductance (*K*), sap flow (*Q*) and shoot biomass growth (*G*) was generally supported. Across species, however, trees grew more for a given *K* or *Q* than shrubs, indicating greater growth-based water-use efficiency (WUE) in trees. Trees also showed slower decline in relative growth rate (RGR) than shrubs, equivalent to a steeper *G* by mass (*M*) scaling exponent in trees (0.77–0.98). The *K* and *Q* by *M* scaling exponents were common across all species (0.80, 0.82), suggesting that the steeper *G* scaling in trees reflects a size-dependent increase in their growth-based WUE. The common *K* and *Q* by *M* exponents were statistically consistent with the 0.75 of ideal scaling theory. A model based upon xylem anatomy and branching architecture consistently predicted the observed *K* by *M* scaling exponents but only when deviations from ideal symmetric branching were incorporated.

Key-words: growth; heat balance method; humidity; metabolic scaling theory; riparian; woody plants; xylem transport.

INTRODUCTION

Studies of plant water transport often assume that greater transport or efficiency of transport leads to greater carbon gain and growth. How valid is this assumption? Theoretically, this idea is based upon the shared stomatal pathway for water loss and carbon gain. Water vapour lost by evaporation induces sap flow, Q, to replace this loss and keep cells hydrated. By Darcy's law, Q is the product of hydraulic conductance, K, and the transport driving force, ΔP : $Q = K\,\Delta P$. For a given ΔP, increasing K by making the xylem network more efficient will support more leaves and/or allow the stomata to open wider, which will increase Q and the potential for CO_2 assimilation. This theory is generally consistent with the observed rates of assimilation and growth. Assimilation decreases when hydraulic conductance is reduced by cutting roots or embolizing the xylem (Wan *et al*. 1993; Hubbard *et al*. 2001). Growth, measured as basal area increment, increases with K and Q (Pataki *et al*. 1998; von Allmen *et al*. 2012). Rootstocks that produce larger fruit trees also have higher K and wider xylem vessels (Solari *et al*. 2006; Tombesi *et al*. 2010). Less direct evidence is shown by exponential increases in K and mass over time (Tyree *et al*. 1998) and studies in which growth and water use generally respond in the same direction to experimental treatments (Grewal 2010; Wolken *et al*. 2011). In this paper, our basic goal is to evaluate the relationship between biomass growth rate, G, and both K and Q. The K represents a plant's structural investment in water transport, whereas Q can be more meaningful for explaining growth when ΔP changes within or across species.

The coordination between growth and hydraulic conductance is a key component of metabolic scaling theory (MST; West *et al*. 1999), wherein the nature of this relationship affects numerous downstream predictions about plant and community scaling. G versus K may be described by the power function,

$$G = a_1 K^{b_1}, \tag{1}$$

with scaling multiplier a_1 and exponent b_1. MST predicts isometry (i.e. $b_1 = 1$) across species. The link from K to G and the prediction of isometry involves assumptions about how K and G scale with Q. Specifically, isometry is required in

$$Q = a_2 K^{b_2} \tag{2}$$

and

$$G = a_3 Q^{b_3}. \tag{3}$$

As per Darcy's law, a_2 and b_2 in Eqn 2 describe how ΔP varies with K. A constant ΔP makes $b_2 = 1$ and $a_2 = \Delta P$, which requires that as plants grow in height, they compensate for the increasing effects of gravity. In Eqn 3, coefficients a_3 and b_3 integrate instantaneous water-use efficiency (WUE) and carbon allocation and how they vary with Q. If instantaneous

Correspondence: D. D. Smith. Fax: + 1 801 581 4668; e-mail: duncan.smith@utah.edu

© 2014 John Wiley & Sons Ltd

WUE is constant and a constant portion of fixed carbon is allocated to growth, then $b_3 = 1$ and a_3 will equal G/Q: a proxy for growth-based WUE.

Assuming, as a null hypothesis, that $b_1 = b_2 = b_3 = 1$ across species, how G, Q and K scale individually with mass, M, may differ interspecifically. These relationships can be written as

$$K = a_4 M^{b_4}, \quad (4)$$

$$Q = a_5 M^{b_5} \quad (5)$$

and

$$G = a_6 M^{b_6}. \quad (6)$$

If isometry exists in Eqns 1–3, then $b_4 = b_5 = b_6$ within species. In MST, the classic prediction is that these 'metabolic' exponents equal 0.75 (West *et al*. 1999). Three-quarter power scaling has since been revised as an upper limit for symmetrically branching trees, based upon the effects of finite size and the observed taper and packing of xylem conduits (Savage *et al*. 2010; Sperry *et al*. 2012). Recently, however, it has been demonstrated that ontogenetic deviation from symmetric to asymmetric branching and the corresponding elongation of crown shape – as observed in young trees – can drive the exponent back up to 0.75 and beyond; this trend is reversed as trees mature and crowns become more spherical (Smith *et al*. 2014).

Metabolic scaling may also be coordinated with species stature (Sperry *et al*. 2012). The role of water transport in limiting the maximum size of trees has received much attention (Ryan *et al*. 2006), but coordination of hydraulic scaling and species-specific stature and growth has not been explored in depth. Taller species may put more of a premium on maximizing the increase in water transport with size and in converting carbon into height growth than smaller statured species. Hence, it has been speculated that taller statured species may have steeper metabolic and hydraulic scaling than shorter statured species (Sperry *et al*. 2012).

In this paper, we determine the empirical scaling relationships in Eqns 1–6 for six co-occurring woody species ranging in stature from shrubs to trees. We chose a riparian community to minimize effects of soil moisture and focused on deciduous diffuse-porous angiosperms to minimize differences in growing season length and xylem anatomy. We evaluate the null hypothesis of isometric scaling between plant hydraulic conductance (K), midday sap flow (Q) and annual shoot biomass growth rate (G). These data allow us to estimate the ranking of growth-based WUE among the species. We test the null hypothesis that hydraulic (K and Q) and metabolic (G) scaling with mass is common across species and is not different from 0.75 as proposed by classic metabolic scaling theory. We compare our empirical K by M exponent (b_4) with model predictions based upon the xylem anatomy of each species and estimate the importance of deviation from symmetric branching (Smith *et al*. 2014). Finally, we investigate the coordination between scaling relationships, WUE ranking and species stature.

MATERIALS AND METHODS

Location and species

The study took place in Red Butte Canyon Research Natural Area (40.8°N, 111.8°W), located adjacent to the University of Utah in Salt Lake City, UT, USA. Measurements were made at elevations between 1642 and 1913 m a.s.l. We chose six species from those in and near the riparian zone, including three shrubs (*Amelanchier alnifolia* Nutt., *Cornus sericea* L. and *Symphoricarpos oreophilus* A. Gray) and three trees (*Acer grandidentatum* Nutt., *Betula occidentalis* Hook. and *Populus fremontii* S. Watson). The shrub versus tree distinction is somewhat subjective so we generally compare species in order of increasing maximum size observed in the study area. All species are angiosperms with simple, deciduous leaves. Their xylem is diffuse-porous, with the exception of *Symphoricarpos*, which we found in the course of the study to be functionally ring-porous (i.e. only the current year's growth ring was conductive.

Whole-plant hydraulic conductance

We measured whole-plant hydraulic conductance, K, in 13–22 plants per species ($n = 98$ in total). K was obtained from sap flow, Q, and xylem pressure, P, measurements made between 11 July and 3 September 2011. Q was measured using the heat balance method (Baker & Van Bavel 1987), in which a sensor containing a heater and various thermocouples is wrapped around each plant trunk. Power from the heater, W_H, may be dissipated radially through the sensor, W_{rad}, or axially by either thermal conductance of the stem, W_{ax}, or convection by sap flow, W_Q. Power may also be stored by the stem, W_s, which is measured by adding another thermocouple to the sensor (Grime *et al*. 1995). W_Q and, hence, Q may be calculated from the power balance:

$$W_Q = W_H - W_{rad} - W_{ax} - W_s. \quad (7)$$

We calculated each component of the power balance using standard procedures. Of note, however, W_{rad} requires the thermal conductance of the sensor sheath, k_{sh}, which varies between installations so it is calculated using Eqn 7 when W_Q is zero. We assumed that W_Q was zero between midnight and 0600 h and calculated k_{sh} when the radial temperature difference was greatest, after removing spurious peaks.

We used seven different Dynagage sap flow sensors (Dynamax, Houston, TX, USA), which accommodated trunk diameters between 8 and 203 mm. Sensors were read every 10 s and averages stored every 10 min using a CR7 datalogger (Campbell Scientific, Logan, UT, USA). Heater voltages were maintained at the manufacturer's recommendation with adjustable regulators (Dimension Engineering, Akron, OH, USA). Concurrent with sap flow measurements, we recorded air temperature and vapour pressure deficit (VPD).

Sap flow sensors were generally installed over a 3 d period, giving one full day and two partial days of measurement. Installations were timed such that the full day occurred when

the weather was warm and sunny, so as to maximize Q. These short installation times allowed for many measurements from several sites during one summer. On 'full' days, the xylem pressure, P, of each individual was measured at pre-dawn (PD) and midday (MD) using a Scholander-type pressure bomb (PMS Instrument Co., Albany, OR, USA). The $P_{PD} - P_{MD}$ is the pressure difference required to induce flow and resist gravity. The gravity component, ρgH, was calculated using the density of water, gravity and plant height, respectively. We recorded the times at which P was measured and calculated mean Q over these times ± 1 h to get Q_{PD} and Q_{MD}. On one occasion, the sensor readings at PD and MD were lost. Because this occurred over a 4 d installation, we assumed P measurements from one day were similar to the following day, which had similar weather. On another occasion, two trunk thermocouples were not working during PD, which prevented us from calculating Q during this time. Therefore, we used Q_{PD} from the following day and assumed P_{PD} had not changed. The ratio of sap flow and xylem pressure differences yields K:

$$K = \frac{Q_{MD} - Q_{PD}}{P_{PD} - P_{MD} - \rho gH}. \quad (8)$$

The numerator shall henceforth be referred to as Q. The denominator is the driving force for sap flow, ΔP. We assessed whether ΔP varies within each species, which is relevant for determining if K scaling is representative of Q scaling.

After measuring K, we used a potometer to test the accuracy of our sap flow sensors on a subset of plants. In total, 23 plants with basal diameters ca. <4 cm were cut underwater using a split funnel and immediately placed in a container with a pre-measured volume of 20 mM KCl solution filtered to 0.2 μm. Plastic wrap was placed across the container opening to reduce evaporation. After transpiring for at least 2 h, the shoot was removed and the remaining solution volume was measured. The average flow rates measured by the sensor and the potometer were compared.

Estimating aboveground growth

We estimated G in nearly all plants used to measure K (n = 87:13–17 per species). We estimated aboveground vegetative growth only. Because our species were deciduous, we defined G (g year^{-1}) as the annual stem mass increment plus the standing leaf mass. Using trunk diameter (D_T), growth ring thicknesses and species-specific allometric relationships, we estimated G as follows.

1 From each measured D_T, we predicted the cambium diameter, D_c, using regressions on D_c versus D_T data. These data came from trunks for which we measured sapwood area (see the section Modelling hydraulic scaling from structure). We subtracted growth ring thickness from each D_c to get the cambium diameter in the previous year. Ring thicknesses were measured from dissecting scope and microscope photos of trunk cross sections and cores. Cross sections were obtained immediately after K measurements, whereas cores were taken later in the season. In both cases, we assumed that most radial growth was already complete for the season. We then predicted D_T in the previous year from its D_c and the D_c versus D_T regressions. This method accounts for changes in D_T due to both xylem and bark.
2 Plant heights, H, in the current and previous years were predicted from H versus D allometry. We constructed H by D curves for each species using whole plants (n = 185, including many used for K), branches (n = 216, from K-plants) and twigs (n = 203, from non K-plants). H measurements were made directly or using trigonometry for taller plants. This dataset was meant to include the full range of plant sizes for each species. As such, we used the maximum D_T from this dataset to define each species stature. The data were fitted with the equation:

$$H = a_7 D^{b_7} - l_o. \quad (9)$$

The l_o term is used because H by D relationships generally start out steep on a log scale and gradually asymptote towards a constant, shallower slope, b_7 (McMahon & Kronauer 1976; Smith *et al*. 2014).
3 Next, dry stem mass, M_{st}, in the current and previous years was predicted from how M_{st} scaled with a shoot volume proxy, HD_T^2. We obtained M_{st} by HD_T^2 scaling from branches (n = 209) and a few K-plants cut down (n = 5), which were oven dried at 60 °C for at least a week.
4 Finally, we predicted total dry leaf mass, M_{lv}, in the current year from M_{lv} versus M_{st} scaling relationships. These relationships came from the same dataset used in step 3 (n = 211 branches; n = 5 whole shoots). We calculated growth as the annual M_{st} increment plus the current M_{lv}.

Modelling hydraulic scaling from structure

Whole-plant hydraulic conductance is largely dependent upon xylem conduit properties and branching structure (Sperry *et al*. 2012; Smith *et al*. 2014). To help interpret our K data in terms of contributions from the xylem and branch networks, we modelled aboveground xylem networks using measured diameters and numbers of active xylem conduits in all species. We used these data to predict aboveground K and used a root:shoot resistance ratio to predict belowground and whole-plant K. Xylem anatomy data were obtained using our own measurements and published data for *A. grandidentatum* collected from the same area (von Allmen *et al*. 2012). We collected xylem samples from a wide range of stem diameters, D. From these samples, thin transverse sections were prepared with a sliding microtome, stained with 1:1 phloroglucinol (1% in EtOH): HCl (12 M), and photographed for analysis. Using at least three photos from each stem, a section of the youngest growth ring was isolated. The area of this xylem section (A_x) and all individual vessel diameters, $\dot{d}$, were measured using STEM GUI software (Charles A. Price, personal communication). From these measurements, we calculated the hydraulically weighted mean vessel diameter $\left(d = \left[\frac{1}{n} \sum_{i=1}^{n} \dot{d}_i^4 \right]^{\frac{1}{4}} \right)$ and the vessel frequency (n/A_x) of each stem (Savage *et al*. 2010).

Combined with stem diameter measurements, these data give vessel taper (d versus D) and packing (n/A_x versus d). Packing data were fitted with power functions. A rise-to-max function was more appropriate for the taper data:

$$d = \frac{Dd_{max}}{D+m}. \quad (10)$$

The d_{max} and m are the fitting parameters. Taper and packing equations together can predict the diameter and number of vessels as a function of stem diameter.

To determine which vessels are functional in water transport, we introduced dye to transpiring stems. Again, we chose a wide range of stem diameters from each species. For small stem diameters (ca. <4 cm), stems were cut underwater using a split funnel and the cut end immediately placed in 0.05% safranin O solution and allowed to transpire for 2 h. Stems were later cut and photographed ca. 10 cm from the end and the dyed area was measured. For larger stems, a hole was drilled at least half way into the trunk. To minimize air introduction to the xylem while drilling (but see Wheeler *et al.* 2013), a modified PVC pipe fitting was secured against the trunk at the drill site and filled with water. Plastic tubing was inserted into the hole and kept filled with safranin O solution as the plant transpired. After at least an hour, a core was taken ca. 10 cm above the dye point using a 5 mm increment borer. Sapwood depth was measured from the cores and converted into sapwood area. All sapwood measurements from small stems and many from larger stems came from plants used for hydraulic conductance measurements.

To obtain root:shoot resistance ratios, we measured midday root crown xylem pressures (P_{RC}) in addition to predawn and midday leaf P. Root crown P was determined by covering a basal shoot with aluminum foil and a plastic bag and measuring its xylem pressure after allowing at least an hour to equilibrate with the root crown. These measurements were obtained from some of the plants used for K as well as others measured in August and September 2013. The proportion of total resistance due to the roots, Pr_{root}, is

$$Pr_{root} = \frac{P_{PD} - P_{RC}}{P_{PD} - P_{MD}}. \quad (11)$$

If Pr_{root} is size-dependent, then whole-plant hydraulic scaling can differ from aboveground scaling (Martínez-Vilalta *et al.* 2007; Sperry *et al.* 2012). We used taper, packing, sapwood and Pr_{root} in a version of the West, Brown & Enquist (WBE) (West *et al.* 1999) model modified by Smith *et al.* (2014). Briefly, this model follows biomechanical rules to create trees that are 'plumbed' with xylem conduits to calculate hydraulic conductance of the stem network. Conduits in leaves and roots are not explicitly modelled. Rather, proportionality constants link their hydraulic conductances to those of the twigs and shoot, respectively. The hydraulic conductances of leaves, stems and roots are added serially to predict K. Aside from adding our species-specific xylem parameters, we only changed the model to accommodate the rise-to-max taper function (Eqn 10).

The model creates plants with either symmetrical WBE architecture or random branching across the spectrum of possible architectures (see Smith *et al.* 2014). Architecture is quantified using the 'path fraction', P_f, which is the ratio of the mean and maximum trunk-to-twig path lengths. The maximum P_f is 1, which corresponds to symmetrical branching and a round crown shape. Smaller P_f values are due to asymmetric branching and result in elongated crown shapes. We modelled hydraulic conductance under two scenarios: constant symmetric WBE architecture ($K_{m,WBE}$) and ontogenetically changing architecture ($K_{m,\Delta}$). In both scenarios, we modelled plants across the measured D_T range of each species. The D_T increments were chosen based upon the discrete diameters possible for WBE structures. The M was predicted from D_T using species-specific allometry as mentioned earlier. For $K_{m,WBE}$, we modelled WBE structures and plumbed them for each species to calculate hydraulic conductances. The modelled points were fitted with a spline to predict $K_{m,WBE}$ at each measured D_T. These predictions were used to test for species differences due to xylem anatomy alone. For $K_{m,\Delta}$, Smith *et al.* (2014) estimated that P_f would start high in small plants, decline rapidly and then increase gradually (see dashed curve in their Fig. 3). In order to model structures that follow this P_f trajectory, we generated 5000 random branching structures at each D_T using the default branching inputs of the model. We then selected structures that matched each target $P_f \pm 0.01$. Five thousand was deemed sufficient to populate the range of possible architectures and resulted in 49–125 structures being chosen at each P_f. Each branching structure was then plumbed for each species according to its anatomy. These predictions were used to test if size-linked variation in branching architecture could be a component of observed K by M scaling results.

Statistics

All analyses were performed within the R modelling and data analysis environment (R Core Team 2014). Unless otherwise noted, all claims of significance were evaluated using $P = 0.05$ as the threshold. For linear regressions, we followed the advice of Warton *et al.* (2006) on when to use OLS (ordinary least squares) or SMA (standardized major axis). In short, when the goal was to predict y data from x data, OLS was used. When the slope of a relationship was of interest, SMA was used. SMA regressions were made and compared using the SMATR package for R (Warton *et al.* 2012). We generally evaluated regressions by testing for common exponents and common multipliers. In the context of this study, the common exponent test considers whether regression lines fit to each species are statistically parallel to each other (on a log-log scale) regardless of their multipliers (see Supporting Information Fig. S1). For the common multiplier test, multipliers are obtained by forcing each regression to follow the common exponent. These 'forced multipliers' are then tested for significant differences. Because comparing multipliers requires use of a common exponent, this test is only relevant when a common exponent is supported (Warton *et al.* 2006). When exponents are

Table 1. Species properties and OLS (ordinary least squares) regressions used for mass prediction

		Local max	H versus D				M_{st} versus HD^2			M_{lv} versus M_{st}		
Species	Growth form	D_T	a_7	b_7	l_o	r^2	Mult	Exp	r^2	Mult	Exp	r^2
Populus fremontii	Tree	76.1	178	0.643	76.0	0.97	0.356	0.99	0.95	1.07	0.88	0.67
Acer grandidentatum	Tree	21.1	191	0.597	75.1	0.98	0.358	1.02	0.99	1.47	0.67	0.79
Betula occidentalis	Tree	21.0	266	0.549	99.4	0.98	0.315	1.01	0.99	0.98	0.73	0.79
Amelanchier alnifolia	Shrub	5.9	160	0.795	37.2	0.96	0.411	0.97	0.98	0.81	0.67	0.75
Cornus sericea	Shrub	3.1	135	0.979	13.1	0.92	0.308	1.01	0.95	1.70	0.56	0.66
Symphoricarpos oreophilus	Shrub	2.5	122	0.776	18.0	0.92	0.531	0.97	0.95	0.67	0.59	0.68

Equations correspond to D and H in centimeters and M in grams. Data are shown in Supporting Information Figs. S3–S5. Species are listed in order of decreasing stature. $P < 0.001$ for all relationships.

different, scaling relationships cross, and multipliers are not indicative of the relative heights of the relationships.

Where appropriate, we compared the exponents and multipliers of individual species using post-hoc pairwise comparisons. When comparing means between species, we used ANOVA to detect differences and used Tukey's Honest Significant Differences for post-hoc pairwise comparisons. The P-values from all pairwise comparisons were adjusted to avoid type I errors.

In this study, we compared a number of plant properties that are autocorrelated. For example, we tested Q versus K scaling when K is calculated from $Q/\Delta P$. However, it should be noted that autocorrelation does not detract from the goals of our analyses. The point of Q versus K analyses was to show the effects of ΔP variation within and between species. Similarly, we analyse G versus M, although M was used as part of G estimation. The G versus M analyses were meant to illustrate the net effect of different growth ring thicknesses and different allometric relationships used to predict mass.

RESULTS

Sap flow sensor accuracy

We compared average flow rates measured simultaneously by sap flow sensors (Q_{sens}) and a potometer (Q_{pot}). One of the 23 measurements was removed because the potometer ran dry. The Q measurements were well correlated ($r^2 = 0.93$; Supporting Information Fig. S2). A SMA regression of Q_{pot} versus Q_{sens} indicated a slightly but significantly greater slope than one (1.17; $P = 0.01$) but the intercept (–2.47e–3) did not differ from zero. These results indicate that the sensors are reasonably accurate but tend to underestimate actual Q by a constant factor.

M, *H* and *D* allometries for predicting growth

We predicted aboveground annual growth, G, using growth ring measurements and four allometric relationships for each species. Cambium versus trunk diameter scaling was very similar across species and data were well correlated within species ($r^2 > 0.98$; not shown). Using these relationships, bark growth was estimated as 1–12% of D_T growth. The H versus D data were fairly convergent across species and each was well fitted by Eqn 9 ($r^2 > 0.92$; Table 1; Supporting Information Fig. S3), which we used to predict H from D_T in the current and previous years.

We used HD_T^2 to predict total dry stem masses, M_{st}, using M_{st} versus HD^2 data. These data were well fitted by power functions ($r^2 > 0.94$; Table 1; Supporting Information Fig. S4), and as expected, M_{st} versus HD^2 relationships were more log-linear than M_{st} versus D^2 or H alone (not shown). Finally, we predicted dry leaf mass, M_{lv}, in the current year using regressions from M_{lv} versus M_{st} data ($r^2 > 0.65$; Supporting Information Fig. S5; Table 1). The good fits observed for each of these allometries gave us confidence in using them to estimate M and G.

Growth by conductance scaling (Eqn 1)

Growth and hydraulic conductance were generally convergent across species. Scaling exponents, b_1, were significant in all but *Symphoricarpos* (Fig. 1a; Table 2). Significant exponents ranged from 0.84 to 1.19 and r^2 from 0.56 to 0.91. Our null hypothesis of isometry was supported by all species, although *Populus* was weakly steeper ($b_1 = 1.19$; $P = 0.052$). Significant species supported a common exponent ($b_1 = 1.06$) that also agreed with isometry. Regressions were forced to the common exponent to compare multipliers. These 'forced multipliers' were not common across species. Additionally, there was a tendency for forced multipliers to increase with increasing species stature, meaning that larger species tended to have greater growth per K than smaller species. The multiplier of the largest statured species, *Populus*, significantly exceeded *Betula* and *Cornus* (see Fig. 1a). Consistent with stature-linked increases in the multiplier, the interspecific scaling exponent across all species ($b_1 = 1.18$) was significantly steeper than isometry (Table 2).

Water use by conductance scaling (Eqn 2)

The Q by K scaling exponents, b_2, were significant in all species, ranging from 0.85 to 1.12 (Fig. 1b; Table 2). None differed from our null hypothesis of isometry, although *Populus* was weakly steeper ($b_2 = 1.12$; $P = 0.051$). Species

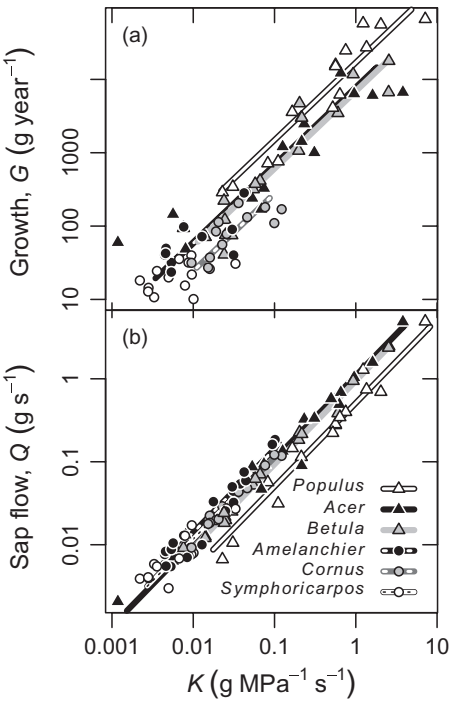

Figure 1. Scaling of aboveground growth and midday sap flow with whole-plant hydraulic conductance. Symbols represent each plant from shrub (circles) and tree (triangles) species. The legend lists species in order of decreasing species stature. (a) All species except *Symphoricarpos* had significant G versus K scaling. The remaining species shared a common SMA (standardized major axis) exponent (0.98). When regressions were forced to the common exponent (shown), trees tended to have greater multipliers than shrubs. (b) All species had significant Q versus K scaling and shared a common SMA exponent (1.01). When forced to this common exponent (shown), multipliers tended to decrease with increasing species stature. Non-forced regression coefficients are shown in Table 2.

supported a common exponent ($b_2 = 1.01$) that also agreed with isometry. Isometry corresponds to a constant ΔP within species, which was confirmed by non-significant ΔP versus K scaling exponents (not shown), although the exponent for *Symphoricarpos* (−0.52) was almost significant ($P = 0.06$). When forced to the common Q by K exponent, species did not share a common multiplier. The forced multipliers of the shrubs were all greater than those of trees (see Fig. 1b), meaning that smaller species transported more water per K than larger ones. Statistically, all species exceeded *Populus*, whereas *Amelanchier* and *Cornus* also exceeded *Betula*. Additionally, *Amelanchier* exceeded *Cornus*. The trend in multipliers suggests that larger statured species tended to have lower ΔP. Indeed, the ΔP of *Populus* (0.54 ± 0.05 MPa; mean ± SE) was significantly less than all other species. *Amelanchier* (1.46 ± 0.08 MPa) exceeded all species but *Symphoricarpos* (1.20 ± 0.11 MPa). The interspecific exponent ($b_2 = 0.93$) was significantly shallower than isometry – consistent with the decrease in multipliers with stature.

Table 2. Whole-tree (Q and K) and total aboveground (G and M) SMA (standardized major axis) scaling relationships

	G versus K		Q versus K		G versus Q		K versus M		Q versus M		G versus M		G/M versus M		$K_{m,WBE}$ versus M		$K_{m,A}$ versus M	
Group	a_1	b_1	a_2	b_2	a_3	b_3	a_4	b_4	a_5	b_5	a_6	b_6	Mult	Exp	Mult	Exp	Mult	Exp
Populus fremontii	1.93e4	1.19[a]	0.57	1.12[a]	3.50e4	1.06	1.31e−4	0.82	2.53e−5	0.92[b]	0.46	0.98[b]		ns	7.32e−4	0.73	8.65e−4	0.75
Acer grandidentatum	4.76e3	0.84	1.00	0.96	4.70e3	0.87	4.21e−5	0.90[b]	6.02e−5	0.87	0.90	0.78	1.38	−0.27	4.50e−4	0.69[c]	2.08e−4	0.82
Betula occidentalis	8.01e3	1.12	0.93	1.00	8.68e3	1.12	2.34e−4	0.75	2.20e−4	0.75	0.69	0.84[b]	1.24	−0.23	2.64e−3	0.65[c]	2.56e−3	0.71
Amelanchier alnifolia	3.16e3	0.86	1.84	1.07	2.41e3	0.87	1.75e−4	0.74	1.83e−4	0.79	1.56	0.69	4.26	−0.49[b]	1.98e−3	0.56[c]	1.74e−3	0.68
Cornus sericea	2.07e3	0.94	1.14	1.00	1.83e3	0.93	3.95e−4	0.78	4.35e−4	0.78	1.35	0.73	2.77	−0.40[b]	2.76e−3	0.62	2.56e−3	0.69
Symphoricarpos oreophilus		ns	0.54	0.85		ns		ns		ns	0.65	0.72	3.75	−0.65[b]	1.85e−3	0.52[c]	1.39e−3	0.68
Common	–	1.06	–	1.01	–	1.03	–	0.80	–	0.82	–	–	–	–	–	–	–	–
Interspecific	1.00e4	1.18[b]	0.80	0.93[b]	1.40e4	1.28[b]	1.58e−4	0.79	2.41e−4	0.74	0.33	0.95[b]	1.19	−0.23	1.09e−3	0.68	1.11e−3	0.74
MST prediction		1		1		1		0.75		0.75		0.75		−0.25		0.75		0.75

Equations correspond to G in g year^{-1}, K in g MPa^{-1}s^{-1}, Q in g s^{-1} and M in g. Data are shown in Supporting Information Figs. S1–S5. Species are listed in order of decreasing stature.
ns, exponent not significantly different from zero ($P > 0.05$). '–', common exponent or multiplier not supported ($P < 0.05$). Significant differences from metabolic scaling theory (MST) predictions denoted as: [a]$P < 0.1$; [b]$P < 0.05$ (modelled results were not tested). [c]K versus M exponent different from modelled ($P < 0.05$).

Environmental variation

Environmental conditions were fairly consistent across measurement days and generally had a minimal influence on Q by K scaling. Midday VPD ranged from 1.2 to 2.7 kPa with no significant trend over time. Residuals of Q versus K increased significantly with midday VPD for *Amelanchier* ($r^2 = 0.32$). Although, *Amelanchier's* Q versus K relationship had $r^2 = 0.94$, suggesting the magnitude of the VPD effect was small. Midday air temperature ranged from 21 to 29 °C. A significant downward trend over time was observed but this was attributed to two cooler late-season days, whose removal nullified the significance ($P = 0.96$). Residuals of Q versus K increased significantly with midday air temperature in *Amelanchier* ($r^2 = 0.45$) and *Symphoricarpos* ($r^2 = 0.53$). These species had respective Q versus K r^2 values of 0.94 and 0.73, again suggesting minor influence of environmental variation on the Q by K scaling. Soil moisture, as assessed by pre-dawn xylem pressure (P_{PD}), ranged from −1 to −0.05 MPa with 95% of values between −0.67 and −0.11 MPa. Pressures measured midseason tended to be the least negative and a quadratic polynomial fit with day of year was significant. The Q by K residuals for *Symphoricarpos* increased significantly as P_{PD} became more negative ($r^2 = 0.39$), but again the Q by K r^2 was high (0.73), suggesting a primary influence of K over environmental factors.

Growth by sap flow scaling (Eqn 3) and WUE

Growth versus sap flow exponents, b_3, were significant in all species except *Symphoricarpos* (Fig. 2a; Table 2). Significant exponents ranged from 0.87 to 1.12, and all agreed with the hypothesized isometry. These species shared a common exponent ($b_3 = 1.03$), which also supported isometry. A common multiplier was not supported. Forced multipliers tended to be greater in trees than in shrubs, meaning that trees put on more growth per water use than shrubs. Statistically, *Populus* had a larger multiplier than all other species. *Acer* and *Betula* exceeded *Cornus* as well. Isometry suggests that growth-based WUE (as G/Q) is approximately constant within species, whereas the trend observed among multipliers suggests that G/Q increased with species stature. The mean G/Q was lower in shrubs than in trees, although the only significant difference was between *Populus* and all other species (Fig. 2b). In accordance with stature-correlated multipliers, interspecific scaling ($b_3 = 1.28$) was steeper than any intraspecific exponent and significantly greater than isometry.

Conductance by mass scaling (Eqn 4)

Hydraulic conductance and mass were significantly correlated in all species, except *Symphoricarpos* (Fig. 3, black circles). Significant exponents ranged from $b_4 = 0.74$ to 0.90 (Table 2). These exponents, except that of *Acer* (0.90), supported the classic MST prediction of $b_4 = 0.75$. The significant species also supported a common exponent ($b_4 = 0.80$) that agreed with 0.75. When forced to the common exponent, a common multiplier was not supported. Forced multipliers showed no noticeable trend with stature or other traits. *Cornus* significantly exceeded *Acer*, *Amelanchier* and *Betula*. Consistent with the lack of any trend in multipliers, the interspecific exponent ($b_4 = 0.79$) did not differ from 0.75.

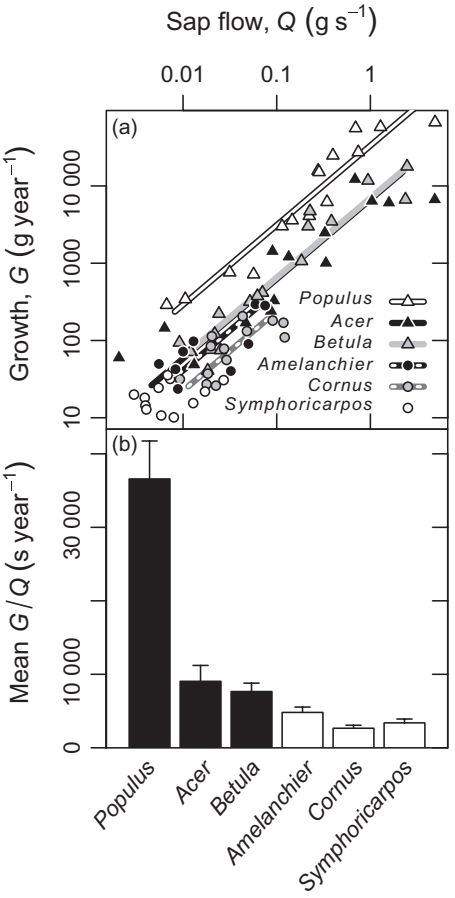

Figure 2. Relationships between aboveground growth and midday sap flow. Species listed in order of decreasing stature. (a) G versus Q scaling was significant in all species but *Symphoricarpos*. Symbols represent each plant from shrub (circles) and tree (triangles) species. Species shared a common SMA (standardized major axis) exponent (0.95). When regressions were forced to the common exponent (shown), multipliers tended to be greater in larger species. (b) Likewise, the water-use efficiency proxy, G/Q, was larger in larger statured species. Shown are the mean $G/Q \pm$ SE with bar colour differentiating trees and shrubs. Non-forced regression coefficients are shown in Table 2.

Sap flow by mass scaling (Eqn 5)

Sap flow and mass were significantly correlated in all species, except *Symphoricarpos*. Significant exponents ranged from $b_5 = 0.75$ to 0.92 (Fig. 4a; Table 2). These exponents, except that of *Populus*, supported the MST prediction of $b_5 = 0.75$. The significant species also supported a common exponent ($b_5 = 0.82$) that agreed with 0.75. A common multiplier was not supported when forced to the common exponent. The forced multipliers of the shrubs tended to be greater than the trees such that shrubs had greater Q at a given mass.

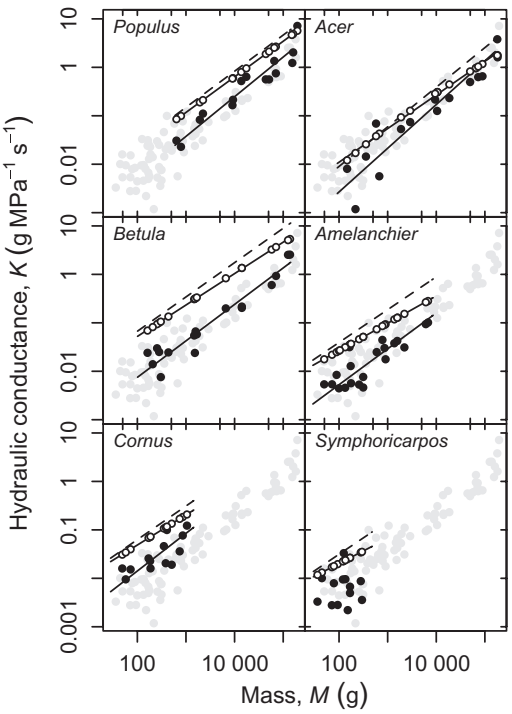

Figure 3. Hydraulic conductance versus aboveground dry mass relationships showing measured K (black circles with solid regression) and K modelled in two ways: either constant WBE branching architecture (open circles with solid regression, $K_{m,WBE}$) or size-dependent branching architecture (dashed regression, data not shown, $K_{m,\Delta}$). In all cases, M was predicted from empirical allometric relationships. For reference, measured data points of all species are shown in grey in the background of each subplot. *Symphoricarpos* had non-significant scaling for measured K versus M. Species displayed in order of decreasing stature. Regression coefficients are shown in Table 2.

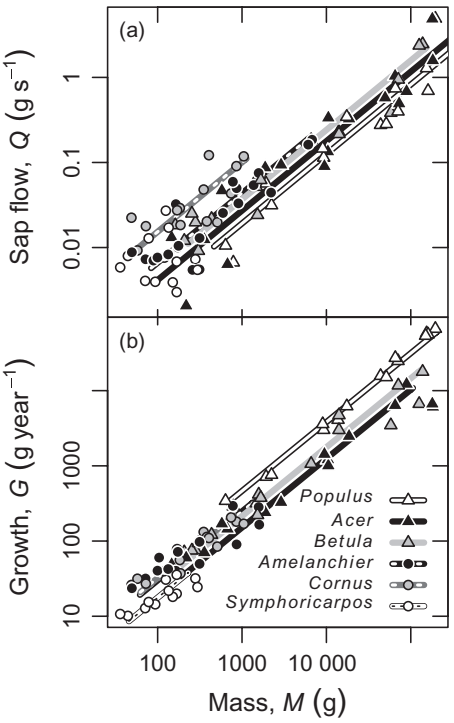

Figure 4. Scaling of midday sap flow and aboveground growth versus aboveground mass. Symbols represent each plant from shrub (circles) and tree (triangles) species. The legend lists species in order of increasing species stature. (a) Q versus M was not significant for *Symphoricarpos*. A common SMA (standardized major axis) exponent (0.82) was supported. When forced to this exponent (shown), trees tended to have smaller multipliers. (b) G versus M scaling was significant in all species. A common SMA exponent was not supported. Trees tended to have steeper exponents than shrubs. Non-forced regression coefficients are shown in Table 2.

Statistically, *Cornus* exceeded all other significant species, whereas *Amelanchier* and *Betula* also exceeded *Populus*. The interspecific exponent ($b_5 = 0.74$) did not differ from 0.75.

Growth by mass scaling (Eqn 6)

Growth and mass were significantly correlated in all species with exponents ranging from $b_6 = 0.70$ to 0.98 (Fig. 4b; Table 2). The MST exponent, $b_6 = 0.75$, was supported by all species except *Betula* and *Populus*. A common exponent was not supported. Shrubs tended to have shallower scaling ($b_6 = 0.70$–0.73) than trees ($b_6 = 0.77$–0.98) but the only significant difference was between trees *Populus* and *Acer*. Interspecific scaling ($b_6 = 0.95$) was significantly steeper than 0.75.

The difference between species is especially apparent when growth is expressed as relative growth rate, G/M (Fig. 5; Table 2). Because b_6 was consistently <1, G/M declined in all species, although not significantly in *Populus*. Among the significant species, a common exponent was not supported. Shrubs tended to have more negative exponents than trees, meaning relative growth rates declined more rapidly. Statistically, *Symphoricarpos* was steeper than *Acer* and *Betula*.

Modelling hydraulic conductance by mass scaling

In each species, we measured xylem anatomy (taper, packing, sapwood) and the proportion of hydraulic resistance in roots, Pr_{root}. From these data, we modelled whole-plant hydraulic conductance using WBE architecture ($K_{m,WBE}$) or changing architecture ($K_{m,\Delta}$) for comparison with K measurements. $K_{m,WBE}$ xylem conduit packing and sapwood measurements were generally well fitted by power functions, whereas a Michaelis–Menten function (Eqn 10) was more appropriate for conduit taper (see Supporting Information Figs. S6–S8; Table 3). Xylem properties were fairly similar between species but with some notable differences. Taper functions indicated that the maximum vessel diameter, d_{max}, ranged from 26 μm (*Symphoricarpos*) to 79.1 μm (*Populus*; Supporting Information Fig. S6). Most packing functions had exponents near −2, indicating a constant xylem fraction devoted to conduits, whereas the exponent of *Symphoricarpos* was much shallower (−1.02; higher vessel frequency in trunks than twigs) and its conduits tended to occupy a larger fraction of the xylem than other species (see Supporting Information Fig. S7). Sapwood area scaling was similar between

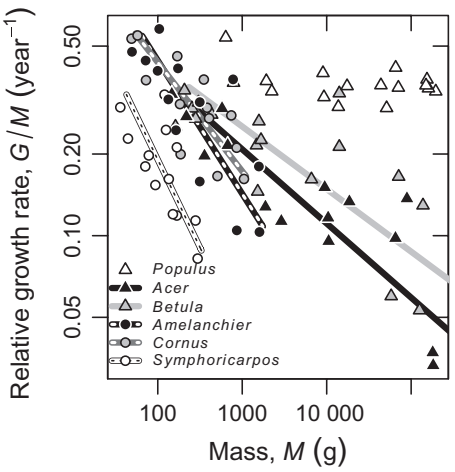

Figure 5. Relative growth rate of aboveground tissue versus current aboveground dry mass. Symbols represent each plant from shrub (circles) and tree (triangles) species. The legend lists species in order of decreasing species stature. Lines indicate SMA (standardized major axis) regressions. The scaling exponents significantly increased with species stature. Moreover, at a given M, larger species tended to have higher G/M. See Table 2 for scaling coefficients.

species, although *Amelanchier* and *Symphoricarpos* had notably less sapwood at a given diameter (Supporting Information Fig. S8). In *Symphoricarpos*, only the outermost growth ring tended to conduct water, which was counter to our assumption that all species were functionally diffuse-porous.

The mean proportion of hydraulic resistance in roots, Pr_{root}, ranged from 0.24 (*Populus*) to 0.50 (*Acer*), but individual measurements varied substantially within each species (overall range: 0.10–0.97; data not shown). The variation was significantly explained by plant size (D_T) in only *Acer* and *Betula*. The Pr_{root} of *Acer* tended to decrease according to a power function ($r^2 = 0.36$), whereas in *Betula*, it tended to increase linearly ($r^2 = 0.29$). For *Acer* and *Betula*, we used these equations to predict Pr_{root} in each plant. For the other four species, we used their respective mean Pr_{root} in determining K_m.

Firstly, we predicted $K_{m,WBE}$ based upon symmetric WBE architecture. The predictions tended to exceeded K measurements (Fig. 3, open circles). The ratio, $K_{m,WBE}/K$, ranged from 0.5 to 14.4 (mean 3.9) with better fit at higher K. The $K_{m,WBE}$ versus M exponents ranged from 0.52 to 0.73 with $r^2 > 0.99$ (Table 2). All exponents were shallower than their measured K versus M counterparts. We treated the modelled exponents as parametric values to test if K versus M exponents differed significantly. Modelled exponents were significantly shallower than measured ones except for *Cornus* ($P = 0.27$) and *Populus* ($P = 0.20$). Thus, using WBE architecture, the model poorly predicted the pattern of scaling variation observed among species.

Next, we predicted $K_{m,\Delta}$ based upon ontogenetically changing architecture (defined as P_f) following estimations of Smith *et al.* (2014). Accordingly, small plants began with P_f near 1 (WBE-type architecture) and dropped to ca. $P_f = 0.4$ before rising gradually again in larger plants. Shrubs occupied the initial P_f-decreasing phase, whereas the study trees extended beyond this phase to where P_f bottomed out and began its gradual rise. The $K_{m,\Delta}$ versus M exponents ranged from 0.68 to 0.82 with $r^2 > 0.99$ (Table 2; Fig. 3, dashed lines). These exponents were steeper than their $K_{m,WBE}$ versus M counterparts but still slightly shallower than measured K versus M exponents. However, all K versus M exponents agreed statistically with $K_{m,\Delta}$ versus M exponents. Furthermore, the modelled and measured exponents were well correlated ($P = 0.005$), suggesting that the model accurately predicted the observed pattern of scaling variation across species when dynamic branching architecture was incorporated.

DISCUSSION

Our main goal was to evaluate the relationship between hydraulic conductance (K) and growth rate (G) in co-occurring woody plants. The data mainly supported the null hypothesis of intraspecific isometry between K and G. Thus, there appears to be an approximately linear connection between water conducting capacity and shoot growth within a species. The data also supported the hypothetical mechanism linking K and G. A size-invariant pressure drop, ΔP,

Table 3. OLS (ordinary least squares) parameters for model input equations

	Taper		Packing		Sapwood	
Species	d_{max}	m	Mult	Exp	Mult	Exp
Populus fremontii	79.1	8.83	1.03e5	–1.66	0.21	2.15
Acer grandidentatum	28.2	2.29	5.77e4	–1.65	1.00	1.84
Betula occidentalis	55.0	4.50	3.54e5	–2.09	0.61	1.99
Amelanchier alnifolia	27.4	1.83	2.97e5	–1.98	0.41	1.89
Cornus sericea	45.5	3.34	1.38e5	–1.78	0.68	1.89
Symphoricarpos oreophilus	26.2	1.41	2.35e4	–1.02	0.38	1.50

Taper is conduit diameter (μm) versus stem diameter (mm). Packing is conduit frequency (mm^{-2}) versus conduit diameter (μm). Sapwood is dyed xylem area (mm^2) versus stem diameter (mm). Taper was fitted with a rise-to-max function (Eqn 10). Power functions are used otherwise. Data are shown in Supporting Information Figs. S6–S8. Species are listed in order of decreasing stature.

resulted in the sap flow rate, Q, being proportional to K within a species. Furthermore, Q was generally proportional to G, implying an approximately size-invariant fraction of assimilated carbon allocated to shoot growth. This proportionality between Q and G, and hence a constant growth-based water-use efficiency (WUE proportional to G/Q), is a basic assumption of vascular-based metabolic scaling theory. Even if G and Q did not scale proportionally with K, the theory in its simplest form would still predict isometry between Q and G. This was indeed the case in *Populus*: G and Q scaled weakly steeper than isometrically with K, yet G and Q remained proportional to each other (Table 2). An exceptional species altogether was *Symphoricarpos*, where many scaling relationships were not significant. However, *Symphoricarpos* was also the smallest species that inherently limited the ability to assess size scaling.

Looking across species rather than within, our results showed a very different trend. Trees tended to grow more for a given K, as shown by their larger forced multipliers (a_1, Eqn 1). The greater growth in trees, however, was not associated with greater sap flow rates. In fact, the opposite trend was observed: trees had lower Q than shrubs at a given K because of a trend to smaller ΔP in trees. The larger species simply grew more for a given Q, which implies greater growth-based WUE. We did not measure WUE because G was measured on an annual basis, whereas Q was a midday average representing maximum seasonal steady-state flow rates. However, the ratio G/Q provides a reasonable WUE proxy if it is assumed that Q is roughly proportional to cumulative seasonal sap flow. This is likely the case as all plants were co-occurring in a riparian setting and had similar leaf phenologies and hence growing season length.

Greater growth-based WUE in trees could result from higher instantaneous WUE (assimilation rate per transpiration rate) and greater allocation of carbon to shoot growth versus other sinks. Greater instantaneous WUE in trees could reflect a greater average exposure of tree canopies to light (Avola *et al*. 2008), although we tried to minimize differences in the light environment of the study plants. From an allocation standpoint, it is likely that trees, particularly in their early years (such as those we sampled), would maximize their shoot growth to reach the canopy, whereas shrubs remain low-growing. Due to the sap flow sensor design, our study trees tended to be small and hence were also rarely fertile. Among the materials used for mass allometry, only 1 of 85 tree branches was reproductive compared to 35 of 126 among shrubs. Reduced allocation to reproduction could favour allocation to shoot growth in trees versus shrubs. Additionally, shrubs may be adapted to more frequent crown disturbances and dieback, and may allocate more carbon to underground storage to facilitate frequent re-sprouting rather than investing heavily in shoot growth (Pate *et al*. 1990; Bowen & Pate 1993; Bond & Midgley 2001). Finally, modelling shows that preferential investment in stems and roots over leaves comes at a metabolic cost, which reduces productivity (Magnani *et al*. 2000). Accordingly, Mencuccini (2003) found that relative to shrubs, trees tended to support more leaves at a given K, which echoes our observations of greater G/Q in trees.

Somewhat surprisingly, given the numerous influences governing metabolic scaling with plant mass (M), our mass scaling exponents (b_4, b_5, b_6) were generally consistent with the classic MST prediction of 0.75. Both K and Q scaled with M to a common exponent that was not statistically different from 0.75 (Table 2). Four of the six species showed a G by M exponent not different from 0.75 (Table 2). According to MST and the observed approximate proportionality between K, Q and G, we expected $b_4 \approx b_5 \approx b_4$. Indeed, the common exponents for K and Q scaling were quite similar ($b_4 = 0.80$ versus $b_5 = 0.82$; Table 2). However, there was more variation in the G by M relationships, which did not support a common b_6 exponent. Interestingly, this G by M exponent increased with species stature (Fig. 4b), such that relative growth rate (RGR) declined much more steeply with plant size in shrubs versus trees (Fig. 5).

In hindsight, it seems obvious that shrubs must have a lower G by M exponent, and hence, faster decline in RGR than trees. After all, if they did not, they would grow to be trees unless they had accelerated annual dieback. This intuitive trend is not, however, demonstrably a consequence of lower Q and K by M exponents in shrubs versus trees as might be expected from MST. Instead, the G by M scaling in a species appears to have changed independently of Q and K. Seemingly, the only way for this to happen is through ontogenetic variation in the WUE proxy, G/Q. Although statistically speaking we found G by Q scaling to be consistent with isometry, the mass scaling observations suggest a statistically non-detected allometry of G/Q. Algebraically, the G/Q by M exponent equals $b_6 - b_5$. In general, this difference is negative in shrubs and positive in trees (*Acer* being an exception). The implication is that growth-based WUE is not only lower in absolute terms in shrubs versus trees as discussed earlier but it also tends to decline with size in shrubs versus increase with size in trees (at least over the size range we measured). These G/Q trends remain hypothetical, however, since they were not statistically evident. Nevertheless, the ultimate outcome of a faster decline in RGR in shrubs versus trees was robust. We are not aware of any studies in which RGR of mature plants was compared between different woody functional types; most observations concern seedlings and emphasize differences between woody and herbaceous growth forms (e.g. Grime & Hunt 1975). Comparisons at the seedling stage for shrubs and trees indicate no difference (Castro-Díez *et al*. 2003), so the divergence we observed may develop later in ontogeny.

Our results provide some insight into the underlying complexity of how woody plant ontogeny results in a particular mass scaling exponent, which, according to ideal MST theory, is similar between b_4, b_5 and b_6. Previous modelling quantifies how the exponents vary with (1) size-dependent trends in WUE and carbon allocation (Enquist *et al*. 2007); (2) the range of sizes being scaled (Savage *et al*. 2010); (3) vascular architecture (Sperry *et al*. 2012); and (4) ontogenetic shifts in branching symmetry (Smith *et al*. 2014). According to our results, any role of (1) should be subtle in our dataset because as previously discussed, G/Q was statistically constant within species. When our model simulations incorporated (2) and

(3) for symmetric crowns (i.e. $K_{m,WBE}$), the modelled metabolic scaling exponent often significantly underpredicted b_4. Moreover, these modelled exponents fell below 0.75, consistent with previous predictions for realistically plumbed trees of finite size and symmetric branching architecture (Savage *et al*. 2010; Sperry *et al*. 2012). However, when we additionally incorporated (4) into the model (i.e. $K_{m,\Delta}$), the scaling exponents steepened, statistically matching b_4. Although the model used the same architectural trajectory for all species, the effect on the modelled exponents varied across species due to differences in xylem anatomy and plant size. Therefore, the combined variation in xylem anatomy and branching architecture appears important for accurately predicting the K by M exponent.

Ontogenetic trends in crown architecture also may explain why our measured K by M exponents were steeper than those measured by von Allmen *et al*. (2012), who found $b_4 = 0.65$ and 0.62, respectively, in *Quercus gambelii* and the same *A. grandidentatum* we measured (and in the same study site). The von Allmen *et al*. study measured a larger range in tree size than we did, up to the biggest trees available. As trees pass out of the juvenile stage and reach the canopy, their crown shape stabilizes and even tends to reverse to a more rounded form (Smith *et al*. 2014). As Smith *et al*. showed, this drives down metabolic scaling exponents. Thus, it is possible that the scaling exponents in the present study differed from those measured by von Allmen *et al*. (2012) because trees were measured over two different architectural phases.

Our observations of approximate isometry between K, Q and G across diverse species strongly support the important idea that the hydraulic network of plants has a strong and simple coordination with carbon assimilation and growth. This validates the long-assumed adaptive significance for the evolution of greater water conducting capacity, and it supports a founding assumption of network-based derivations of metabolic scaling theory. At the same time, our results highlight that growth may be altered independently of water transport. Shrubs in our dataset appeared to grow less for a given water transport capacity than the trees we studied; and the shrubs tended towards flatter growth by mass scaling than young trees. Divergence in instantaneous WUE and allocation presumably create these differences between species. Differences between species and functional types resulted in interspecific scaling being generally different from intraspecific scaling, as will usually be the case (Heusner 1982). Intraspecific scaling is complex, but as our results indicate, it can be predicted from multiple ontogenetic processes and constraints. In contrast, interspecific scaling quickly becomes ambiguous because it depends not only on the scaling for each species involved and species sampling but also on the size range over which each species was measured. Part of the appeal of a species-specific metabolic scaling approach is that K and how it scales may be predicted using a small (but growing) number of structural parameters that can be measured fairly easily for individual species. The Q can then be predicted from standard ΔP measurements or assumptions. Any modelling of G from Q, however, will require capturing the dominant controls on instantaneous WUE and carbon allocation.

ACKNOWLEDGMENTS

We thank Henry Grover and David Love for their field assistance and numerous anatomical measurements. Allison Thompson also contributed to growth ring and sapwood measurements. Helpful input was provided by Lisa Bentley, Brian Enquist, Peter Reich and Van Savage in the early stages of this work. The authors were supported by NSF (Grant No. IBN-0743148). We declare no conflicts of interest.

REFERENCES

von Allmen E.I., Sperry J.S., Smith D.D., Savage V.M., Reich P.B., Enquist B.J. & Bentley L.P. (2012) A species' specific model of the hydraulic and metabolic allometry of trees. II. Testing predictions of water use and growth scaling in species with contrasting hydraulic traits. *Functional Ecology* **26,** 1066–1076.

Avola G., Cavallaro V., Patanè C. & Riggi E. (2008) Gas exchange and photosynthetic water use efficiency in response to light, CO_2 concentration and temperature in *Vicia faba*. *Journal of Plant Physiology* **165,** 796–804.

Baker J.M. & Van Bavel C.H.M. (1987) Measurement of mass flow of water in the stems of herbaceous plants. *Plant, Cell & Environment* **10,** 777–782.

Bond W.J. & Midgley J.J. (2001) Ecology of sprouting in woody plants: the persistence niche. *Trends in Ecology & Evolution* **16,** 45–51.

Bowen B.J. & Pate J.S. (1993) The significance of root starch in post-fire shoot recovery of the resprouter *Stirlingia latifolia* R. Br. (Proteaceae). *Annals of Botany* **72,** 7–16.

Castro-Díez P., Montserrat-Martí G. & Cornelissen J.H.C. (2003) Trade-offs between phenology, relative growth rate, life form and seed mass among 22 Mediterranean woody species. *Plant Ecology* **166,** 117–129.

Enquist B.J., Kerkhoff A.J., Stark S.C., Swenson N.G., McCarthy M.C. & Price C.A. (2007) A general integrative model for scaling plant growth, carbon flux, and functional trait spectra. *Nature* **449,** 218–222.

Grewal H.S. (2010) Water uptake, water use efficiency, plant growth and ionic balance of wheat, barley, canola and chickpea plants on a sodic vertosol with variable subsoil NaCl salinity. *Agricultural Water Management* **97,** 148–156.

Grime J. & Hunt R. (1975) Relative growth-rate: its range and adaptive significance in a loca flora. *The Journal of Ecology* **63,** 393–422.

Grime V.L., Morison J.I.L. & Simmonds L.P. (1995) Including the heat storage term in sap flow measurements with the stem heat balance method. *Agricultural and Forest Meteorology* **74,** 1–25.

Heusner A.A. (1982) Energy and metabolism. I. Is the 0.75 mass exponent of Kleiber's equation a statistical artifact? *Respiration Physiology* **48,** 1–12.

Hubbard R.M., Stiller V., Ryan M.G. & Sperry J.S. (2001) Stomatal conductance and photosynthesis vary linearly with plant hydraulic conductance in ponderosa pine. *Plant, Cell & Environment* **24,** 113–121.

McMahon T.A. & Kronauer R.E. (1976) Tree structures: deducing the principle of mechanical design. *Journal of Theoretical Biology* **59,** 443–466.

Magnani F., Mencuccini M. & Grace J. (2000) Age-related decline in stand productivity: the role of structural acclimation under hydraulic constraints. *Plant, Cell & Environment* **23,** 251–264.

Martínez-Vilalta J., Korakaki E., Vanderklein D. & Mencuccini M. (2007) Below-ground hydraulic conductance is a function of environmental conditions and tree size in Scots pine. *Functional Ecology* **21,** 1072–1083.

Mencuccini M. (2003) The ecological significance of long-distance water transport: short-term regulation, long-term acclimation and the hydraulic costs of stature across plant life forms. *Plant, Cell & Environment* **26,** 163–182.

Pataki D.E., Oren R. & Phillips N. (1998) Responses of sap flux and stomatal conductance of *Pinus taeda* L. trees to stepwise reductions in leaf area. *Journal of Experimental Botany* **49,** 871–878.

Pate J.S., Froend R.H., Bowen B.J., Hansen A. & Kuo J. (1990) Seedling growth and storage characteristics of seeder and resprouter species of Mediterranean-type ecosystems of S.W. Australia. *Annals of Botany* **65,** 585–601.

R Core Team (2014) *R: A Language and Environment for Statistical Computing*. R Foundation for Statistical Computing, Vienna, Austria (URL: http://www.R-project.org/).

Ryan M.G., Phillips N. & Bond B.J. (2006) The hydraulic limitation hypothesis revisited. *Plant, Cell & Environment* **29,** 367–381.

Savage V.M., Bentley L.P., Enquist B.J., Sperry J.S., Smith D.D., Reich P.B. & von Allmen E.I. (2010) Hydraulic trade-offs and space filling enable better

predictions of vascular structure and function in plants. *Proceedings of the National Academy of Sciences of the United States of America* **107,** 22722–22727.

Smith D.D., Sperry J.S., Enquist B.J., Savage V.M., McCulloh K.A. & Bentley L.P. (2014) Deviation from symmetrically self-similar branching in trees predicts altered hydraulics, mechanics, light interception and metabolic scaling. *The New Phytologist* **201,** 217–229.

Solari L.I., Pernice F. & DeJong T.M. (2006) The relationship of hydraulic conductance to root system characteristics of peach (*Prunus persica*) rootstocks. *Physiologia Plantarum* **128,** 324–333.

Sperry J.S., Smith D.D., Savage V.M., Enquist B.J., McCulloh K.A., Reich P.B., . . . von Allmen E.I. (2012) A species' specific model of the hydraulic and metabolic allometry of trees. I. model description, predictions across functional types, and implications for inter-specific scaling. *Functional Ecology* **26,** 1054–1065.

Tombesi S., Johnson S.R., Day K.R. & DeJong T.M. (2010) Relationships between xylem vessel characteristics, calculated axial hydraulic conductance and size-controlling capacity of peach rootstocks. *Annals of Botany* **105,** 327–331.

Tyree M., Velez V. & Dalling J.W. (1998) Growth dynamics of root and shoot hydraulic conductance in seedlings of five neotropical tree species: scaling to show possible adaptation to differing light regimes. *Oecologia* **114,** 293–298.

Wan C., Sosebee R.E. & McMichael B.L. (1993) Growth, photosynthesis, and stomatal conductance in *Gutierrezia sarothrae* associated with hydraulic conductance and soil water extraction by deep roots. *International Journal of Plant Science* **154,** 144–151.

Warton D.I., Wright I.J., Falster D.S. & Westoby M. (2006) Bivariate line-fitting methods for allometry. *Biological Reviews of the Cambridge Philosophical Society* **81,** 259–291.

Warton D.I., Duursma R.A., Falster D.S. & Taskinen S. (2012) Smatr 3 – an R package for estimation and inference about allometric lines. *Methods in Ecology and Evolution* **3,** 257–259.

West G.B., Brown J.H. & Enquist B.J. (1999) A general model for the structure and allometry of plant vascular systems. *Nature* **400,** 664–667.

Wheeler J.K., Huggett B.A., Tofte A.N., Rockwell F.E. & Holbrook N.M. (2013) Cutting xylem under tension or supersaturated with gas can generate PLC and the appearance of rapid recovery from embolism. *Plant, Cell & Environment* **36,** 1938–1949.

Wolken J.M., Landhäusser S.M., Lieffers V.J. & Silins U. (2011) Seedling growth and water use of boreal conifers across different temperatures and near-flooded soil conditions. *Canadian Journal of Forest Research* **41,** 2292–2300.

Received 9 May 2014; received in revised form 3 July 2014; accepted for publication 7 July 2014

SUPPORTING INFORMATION

Additional Supporting Information may be found in the online version of this article at the publisher's web-site:

Figure S1. Distinction between common and interspecific scaling.
Figure S2. Sapflow sensor accuracy testing.
Figure S3. Height by diameter relationships.
Figure S4. Stem mass by HD^2 scaling.
Figure S5. Leaf mass by stem mass scaling.
Figure S6. Xylem conduit taper.
Figure S7. Xylem conduit packing.
Figure S8. Sapwood area scaling.